Highly Accelerated Testing of Capacitors for Medical Applications

Travis Ashburn, Dan Skamser
KEMET Electronics
Simpsonville, SC, USA
travisashburn@kemet.com, danskamser@kemet.com

ABSTRACT
As the market for medical devices continues to grow and expand, it has become evident that product reliability must remain a top priority for medical device manufacturers. In order to guarantee reliability, device manufacturers must choose reliable medical-grade components for their high-reliability applications. Reliability for passive components, especially capacitors, is typically conducted through accelerated and highly accelerated life testing (HALT). Models are used to fit the distributions of insulation resistance to provide prediction capability for lifetime estimates. Risk is minimized by correctly rating the capability (temperature and voltage) of capacitors based on the models. In this paper, Models and Time-to-Failure (TTF) predictions at application conditions for the widely used X7R and C0G ceramic capacitors will be discussed.

INTRODUCTION
The Medical Device market, much like the general electronics market, is continuously pushing for greater functionality while desiring to minimize board space. This technology trend is generally known in the industry as "Moore's Law" and ceramic capacitor technology has continued to keep pace with this trend in miniaturization. Figure 1 illustrates the ever-increasing volumetric efficiency and available capacitance values for the EIA 0603 Class II 6.3V rated MLCC.

Figure 1

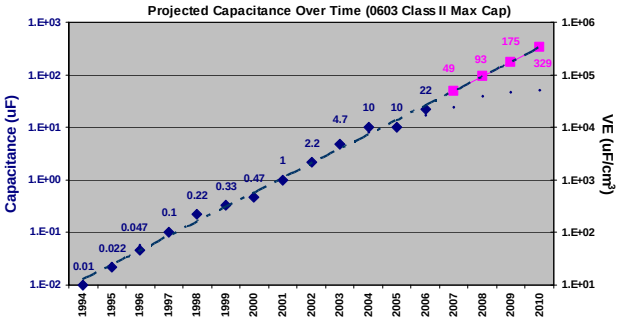

In the 90's, capacitor technology shifted from Precious Metal Electrode (PME) technology to Base Metal Electrode (BME) technology. BME capacitor technology primarily utilizes nickel in the electrode system whereas PME technology utilizes a palladium-silver alloy electrode system. One of the primary advantages of using BME technology is the increased voltage stress capability over traditional PME dielectrics. The increase in voltage stress capability allows for the reduction of dielectric thickness without sacrificing voltage robustness.

Figure 2 illustrates the formula for capacitance and volumetric efficiency of a ceramic capacitor. BME technology enables reduced dielectric thickness, increases in the number of active layers, and increases in the total active area. All of these improving variables significantly contribute to the increased capacitance and volumetric efficiency of ceramic capacitors over time. In keeping pace with the trend in Ceramic capacitor technology, KEMET has recently introduced two high-capacitance C0G and X7R platforms.

Figure 2
Capacitance and Volumetric Efficiency Equations

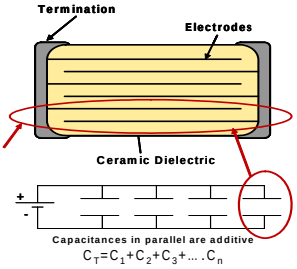

$$C = \frac{e_o K A n}{t}, \quad VE = \frac{C}{V} \sim \frac{e_o K}{t^2}$$

C = Capacitance
VE=Volumetric Efficiency
V=volume
e_o=8.854x10^{-12} F/m
K = Dielectric Constant
A = Overlap Area per active
n = Number of actives
t = Ceramic Thickness

The EIA specification for X7R dielectrics requires that the capacitance variation from the room temperature ($\Delta C/C$) should be within ±15% over the temperature range of -55°C to 125°C. Due to the need for high capacitance with such a controlled temperature variation of capacitance, the X7R dielectrics are based on barium titanate, $BaTiO_3$. Several studies have discussed various aspects of microstructure and properties of X7R Multilayer Ceramic Capacitors (MLCC) [1-4]. Several dopants and additives are added to the barium titanate to achieve the desired capacitance characteristics along with high reliability under bias and temperature conditions. Typical dielectric constants (K) are in the range of 2700 to 3200. In the base metal electrode (BME, usually Ni electrodes) X7R systems, the common dopants and additives include oxides of manganese, alkaline earth elements (Ca, Mg, etc.), rare earth elements, and suitable sintering aids. These additives also play an important role of making the dielectric resistant toward reduction under the $H_2/N_2/H_2O$ atmosphere used during thermal processing of BME MLCC.

There are several key factors involved in achieving high reliability in the X7R dielectric. These include:

1. Choosing a barium titanate
   a. high purity
   b. high crystallinity
   c. controlled particle size
   d. controlled surface area
2. Making a uniform coating of the dielectric
3. Controlling microstructure
4. Optimizing dopants & additives
5. Controlling atmospheric conditions during thermal processing
6. Ensuring a robust end termination process

During the past decade, considerable amounts of research and development efforts have been expended at KEMET and other manufacturers to optimize these and many other parameters to make robust X7R MLCC products.

In applications where capacitance needs to be precisely controlled over a wide temperature range, such as digital tuning and timing, the C0G dielectric is an optimum choice in a MLCC. The EIA specification for C0G dielectric is that the capacitance variation from room temperature (25°C) should be within 0±30 ppm/°C over the temperature range of -55°C to 125°C. Traditional C0G dielectric materials for precious metal electrodes (PME, such as Pd or Ag/Pd) are typically based on the barium neodymium titanate (BNT). The base metal electrode C0G dielectrics (BME, primarily Ni electrode) are $CaZrO_3$-based materials with a dielectric constant (K) of ~31. Compared with PME C0G dielectric, these BME C0G dielectric systems have the additional benefit that they can offer much higher insulation resistance and better reliability (based on HALT and Life Test), and higher Q factor even at thinner dielectric thickness [5-7].

With the recent breakthroughs in coating thin dielectric layers (as thin as ~1 µm) and the capability of stacking hundreds of dielectric layers in BME technology, the volumetric efficiencies of BME C0G MLCCs are increasing significantly. Capacitance values of 1µF will soon be possible in a case size of 2824, along with a 0.68µF in a 2220. The $CaZrO_3$-based dielectric with manganese additive is highly reduction-resistant under the $H_2/N_2/H_2O$ atmosphere used during the thermal processing of MLCCs consisting of Ni-electrodes. As discussed later in this paper, the BME-C0G system demonstrates excellent reliability characteristics at 125°C as well as 150°C.

This paper examines two leading-edge BME C0G and X7R dielectric systems. The HALT testing performed is used to characterize the reliability of the capacitor behavior at accelerated conditions and then in turn used to extrapolate the reliability of the capacitor at typical use conditions. The Prokopowicz and Vaskas (P-V) [8] empirical equation is employed to correlate the reliability behavior at accelerated test conditions to operating conditions. Equation 1 depicts the P-V formula.

Eq. 1

$$\frac{t_1}{t_2} = \left(\frac{V_2}{V_1}\right)^n \exp\left[\frac{E_a}{k}\left(\frac{1}{T_{1_{abs}}} - \frac{1}{T_{2_{abs}}}\right)\right]$$

t_i = time to failure under conditions i
V_i = voltage under condition i
n = voltage stress exponential
E_a = activation energy for dielectric wear out
k = Boltzmann's constant (8.62E-5 eV/K)
T_i = absolute temperature for condition i

The P-V model has been used extensively in experiments and studies on ceramic capacitor reliability [9-12]. Because there are differences in voltage coefficients and activation energies, it is important to characterize each dielectric system across a range of dielectric thickness values and case sizes. This particular study will examine EIA case sizes 0402, 0603, 1206, and 1210 and voltage ratings of 16V, 25V, 50V, and 100V. These voltage ratings and case sizes are commonly used in the electronics industry. Capacitance values range from 1000pF up to 1.0µF depending on dielectric system and case size. Table 1 depicts a summary of the values studied.

Table 1

Dielectric	Case Size	Voltage Rating	Capacitance
X7R	0402	16V	0.1µF
X7R	0603	50V	0.1µF
X7R	1210	100V	1.0µF
C0G	0402	25V	0.001µF
C0G	0603	100V	0.0047µF
C0G	1206	25V	0.1µF

General capacitor design characteristics for the capacitors selected are illustrated in Table 2.

Table 2

Part Description	Breakdown Voltage Mean (V)	Dielectric Thickness (µm)	Electrode Thickness (µm)	Active Layers	Fired Margins (in)	Active Area (in^2)	K Value	Grain Size (µm)
C0G 0402 1nF 25V	750	2.7	1.2	59	0.005	0.0276	30	0.8 to 1.2
C0G 0603 4.7nF 100V	860	3.9	1.2	115	0.006	0.0484	30	0.8 to 1.2
C0G 1206 100nF 25V	650	2.7	1.2	349	0.008	0.1041	30	0.8 to 1.2
X7R 0402 100nF 16V	430	3.2	1.2	66	0.005	0.0276	2800	0.4 to 0.6
X7R 0603 100nF 50V	600	5.1	1.2	45	0.006	0.0476	2800	0.4 to 0.6
X7R 1210 1.0µF 100V	590	10.4	1.2	105	0.008	0.1005	2800	0.4 to 0.6

EXPERIMENTAL METHODOLOGY

It is assumed the mechanism for failure is both thermal and voltage activated following the empirical P-V model. This P-V equation can be simplified to a single function of time.

Eq. 2

$$t = A\, V^{-n}\ \exp[E_a/k\, T^{-1}]$$

A = time constant (min)

This simplified equation can be rewritten in a form that is more useful for experimental modeling by taking the natural log.

Eq. 3

$$\mathrm{Ln}(t) = \mathrm{Ln}(A) - n\,\mathrm{Ln}(V) + E_a/k\,T^{-1}$$

Typically the time (t) used for reliability modeling is the median time to failure, MTTF or t_{50}. Experimental HALT runs are completed to determine MTTF at various combinations of temperature and voltage to map out the model space. The Ln(MTTF) data is fit to the P-V model using a multiple regression computation with predictors Ln(V1) and T^{-1}. Thus the model coefficients of time constant (A), voltage exponent (n) and the activation energy (E_a) are determined. These coefficients are substituted into the P-V equation to estimate time to failure for selected temperature and voltage levels.

In addition to determining the MTTF at selected temperatures and voltages, it is desirable to predict the failures-in-time (FIT) based on the P-V model. The FIT model is used to predict failure rates at different operating conditions based on known application conditions.

Eq. 4

$$FIT = \left(\frac{\#Failures_{Life}}{\#Samples_{Life} * \#Hours_{Life}}\right)\left(\frac{V_{Use}}{V_{Life}}\right)^{\eta}\left(e^{\frac{E_a}{k}\left(\frac{1}{T_{Life}+273.3}-\frac{1}{T_{Use}+273.3}\right)}\right)\cdot(1x10^9)$$

FIT = Failures/Billion Hours @ Use Conditions

V = Voltage (subscripts refer to life test and use conditions)

T = Temperature in Celsius (subscripts refer to life test and use conditions)

n = Voltage Stress Exponential (estimated from HALT Modeling)

E_a = Activation Energy in eV (estimated from HALT Modeling)

K = Boltzmann Constant in eV/K 8.62E-5

EXPERIMENTAL RESULTS

All the HALT experiments were conducted in a commercial oven with maximum capabilities of 600V and 175ºC (Model CE9051, DM511, Micro Burn-in Technologies). The current of the parts was monitored in-situ during the run every 40 seconds. The current limit was set at 100µamps for determining a failure. The sample size was 20 parts per test trial. All test trials were run for 200 hours to generate sufficient data to allow prediction of MTTF.

Analysis of the time-to-failure data was conducted by plotting the data on log plots. Linear fits were applied to the data to determine the MTTF. Figures 3 and 4 show the time-to-failure plots for both the X7R 0402 100nF 16V and C0G 1206 100nF 25V parts. Note that in most cases a linear correlation fit well for all data in the time distribution using regression analysis. However, in some cases there was limited data because less the 50% of the parts failed after 200 hours. For these cases, advanced regression analysis was completed by right-censoring the data with time of 12,000 minutes (parts did not fail in 200 hours). In other cases, where the time distribution showed multi-modes or extended tails, experienced discretion was taken to fit the data that most represented the wear-out behavior. For instance, the data for the X7R 0402 part at 100V in Figure 3 at 125ºC was fit to the lower distribution because it was parallel to the data at 75V. Another example for the C0G 1206 at 100V in Figure 4 at 155ºC, the upper distribution of the time distribution was fit because it was parallel to the data at 75V.

Generally, the slopes of the linear fits were parallel at a given temperature. This demonstrates well-behaved experimental data that is failing due to one mechanism of failure. It is assumed this demonstrates the typical dielectric degradation mechanism of oxygen vacancies piling up along the grain boundaries ultimately leading to wear-out. However, in some cases the slopes are different indicating a change in the failure mechanism. This occurred mainly at the higher voltages, especially in the C0G parts. This likely indicates a different breakdown mechanism of the dielectric with application of extreme voltage stress on the part. Possibly, minor defects such as micro-pores or imperfections become hot spots for localized dielectric degradation due to the increased electric field imposed. The purpose of this paper is not to determine the exact mechanism for dielectric wear-out.

Note that linear fits could not be determined for the C0G 0603 4.7nF 100V part because it was difficult to achieve failure during the HALT testing. Figure 5 shows only two failures occurred at highest temperature (175ºC) and 575V. Unfortunately, the HALT equipment was incapable of more stressful conditions and it was unrealistic to conduct test trials longer than 200 hours.

The MTTF based on the linear estimation fits are shown in Table 3 for each part type. A value of time in minutes is given for selected temperature and voltages. In some cases the number of failures was minimal such that a MTTF could not be estimated. In these cases, just the number of failures is indicated. In all cases the data was well behaved. Again note the C0G 0603 4.7nF 100V part had very few failures except at 175ºC. This shows the robustness of this part type to the testing, indicating a highly reliable part.

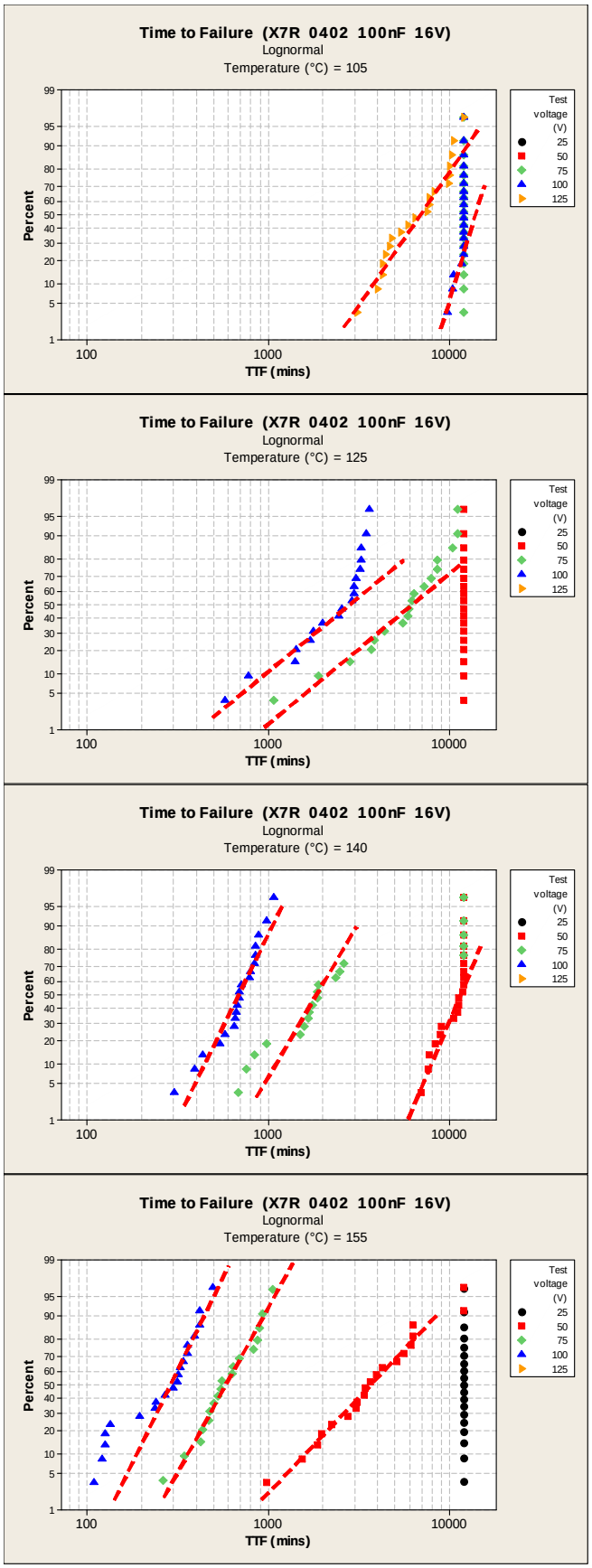

Figure 3: Time-to-failure plots at various temperatures and voltages showing linear estimation fits for the X7R 0402 100nF part.

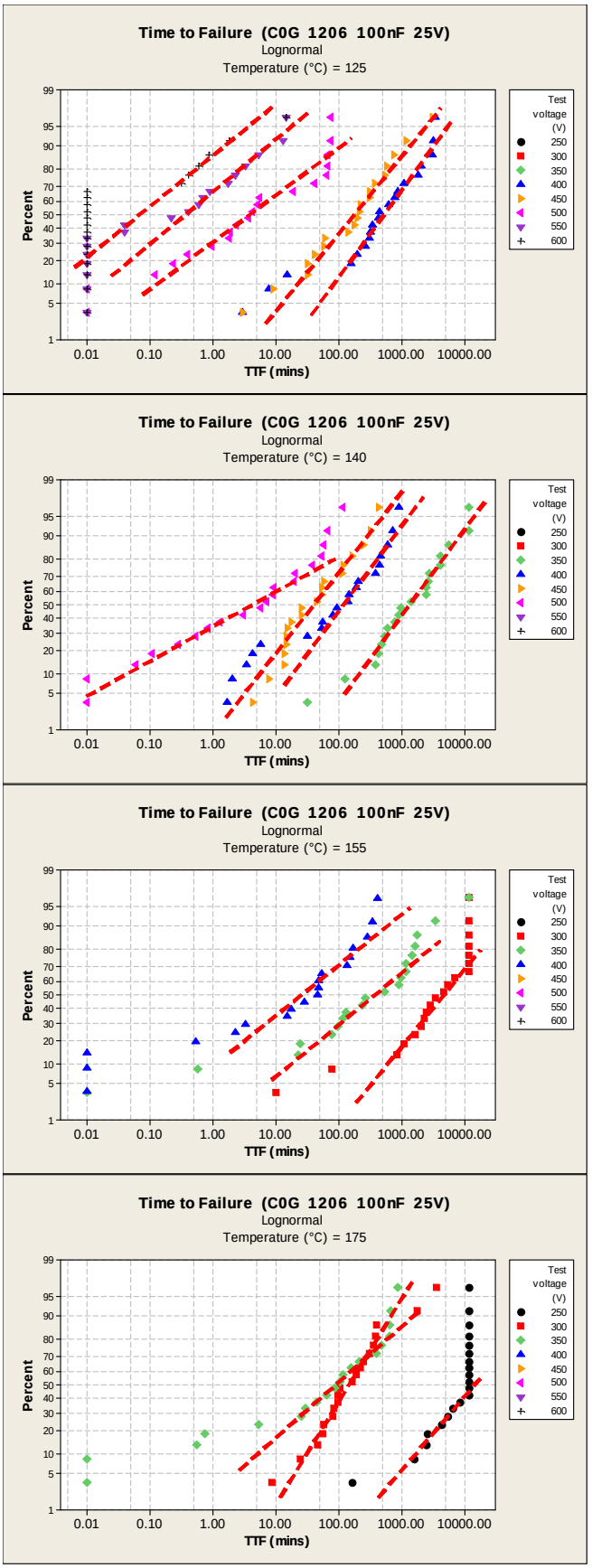

Figure 4: Time-to-failure plots at various temperatures and voltage showing linear estimation fits for the C0G 1206 100nF part.

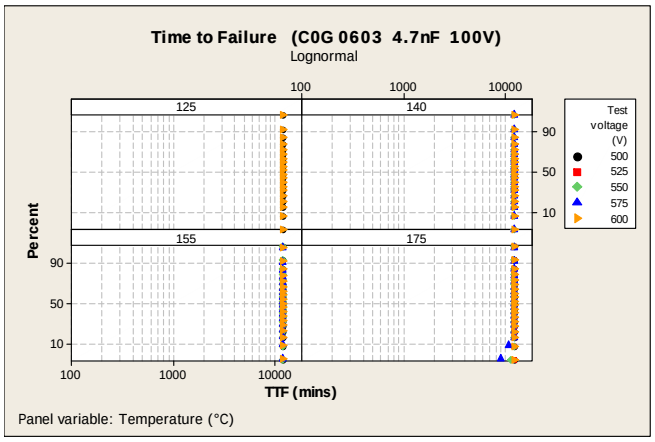

Figure 5: Time-to-failure plots at various temperatures and voltages for the C0G 0603 4.7nF 100V part. Linear estimation fits could not be completed since there were few HALT failures.

Table 3: MTTF for each part type based on linear estimation fits.

		Temperature (ºC)			
Part No.	VOLT	105	125	140	155
X7R 0402 0.1000µF 16V (time in min)	125	5070			
	100	13586	2726	662	307
	75	0 fail	6140	1921	584
	50		0 fail	11495	3638
	25				0 fail

		Temperature (ºC)			
Part No.	VOLT	105	125	140	155
X7R 0603 0.1000µF 50V (time in min)	500	6473	786	287	
	450	14600	2246	467	
	400		5055	990	248
	350		9973	2600	507
	300		3 fail		1558
	200				8555

		Temperature (ºC)			
Part No.	VOLT	105	125	140	155
X7R 1210 1.0000µF 100V (time in min)	450	66383	10639		
	425	0 fail	3 fail	13043	
	400	2 fail	3 fail	16288	
	375	0 fail	1 fail	27230	4966
	350	0 fail	1 fail		10220
	320				35619

		Temperature (ºC)			
Part No.	VOLT	125	140	155	175
C0G 0402 0.0010µF 25V (time in min)	600		365	139	69
	575		437	381	60
	550		1515	663	193
	525				432
	500			3747	760
	150			0 fail	

		Temperature (ºC)			
Part No.	VOLT	125	140	155	175
C0G 0603 0.0047µF 100V (time in min)	600	0 fail	0 fail	0 fail	0 fail
	575		0 fail	0 fail	2 fail
	550		0 fail	0 fail	1 fail
	525				0 fail
	500	0 fail		0 fail	0 fail

		Temperature (ºC)			
Part No.	VOLT	125	140	155	175
C0G 1206 0.1000µF 25V (time in min)	550	0.31			
	500	4.1	2.73		
	450	208	40.7		
	400	447	110	75	
	350		1286	208	98
	300			4129	153
	250				13445

Multiple regression fit of the MTTF data for each part type was conducted to estimate the model coefficients (Table 4). Overall the r^2 was greater than 90% showing a good fit to the P-V model. Only the X7R 1210 1.0µF 100V part had a low r^2, mainly due to the limited amount of MTTF data collected at lower temperatures. Generally, the E_a and n were consistent with those reported by others[9-12]. The C0G dielectrics had high voltage exponents indicating a large voltage dependence. They also had an extremely large time constant suggesting these parts have a long lifetime at benign conditions. The X7R had both time constant and voltage exponents that correlated to the voltage rating. In turn, this correlates well with the dielectric thickness of the corresponding part types (0402: 3.2µm, 0603: 5.1µm, 1210: 10.4µm).

Table 4: Model Coefficients

Part Number	Dielectric Family	Rated Voltage	A (mins)	n	Ea (eV)	r2
0402 100nF	X7R	16	1.16E-03	3.8	1.1	98.3%
0603 100nF	X7R	50	4.43E+01	5.4	1.27	97.5%
1210 1µF	X7R	100	1.31E+13	8.4	1.05	75.4%
0402 1nF	C0G	25	1.11E+37	16.4	0.91	94.9%
1206 100nF	C0G	25	1.02E+30	17.3	1.39	89.7%

The P-V model was used to predict the MTTF at standard conditions (125ºC, $2xV_r$ and $1xV_r$) and in-vitro conditions (37ºC, $1xV_r$ and $0.5xV_r$) shown in Table 5. For X7R, the lifetime is strongly a function of voltage rating (i.e., dielectric thickness). The lifetime at 125ºC and 2xVr is reasonable, but is greatly increased when the voltage is reduced to 1xVr. More importantly, the lifetime at 37ºC at either voltage is nearly infinite compared to the life expectancy of a typical medical device. The lifetime at any conditions for the C0G are realistically infinite. In summary, the likelihood of any of these parts failing under in-vitro conditions is extremely remote.

Table 5: Predicted Median Time to Failure

Part Number	Dielectric Family	Rated Voltage	MTTF (Yrs) 125C 1xVr	MTTF (Yrs) 85C 0.5xVr	MTTF (Yrs) 37C 1xVr	MTTF (Yrs) 37C 0.5xVr
0402 100nF	X7R	16	4.9	2,500	4.4.E+04	6.2.E+05
0603 100nF	X7R	50	599	1,600,000	2.2.E+07	9.4.E+08
1210 1µF	X7R	100	7,734	8.0E+07	4.6.E+07	1.5.E+10
0402 1nF	C0G	25	8.3E+19	1.4E+26	1.5.E+23	1.3.E+28
1206 100nF	C0G	25	5.0E+17	7.5E+24	4.9.E+22	8.0.E+27

In addition to HALT testing, load life tests were conducted under standard environmental conditions of twice rated voltage and 125ºC for 1000 hours. A large sample size ranging from 460 to 1000 pieces was tested for each part type. The limit was set for each part type based on EIA specification. This data will be used in the FIT model for each part type.

Table 6: Load life failures at 125°C and 2xVr.

Part Type	Qty	Test Voltage	100 hrs.	250 hrs.	500 hrs.	1000 hrs.	Total
C0G 0402 1nF 25V	500	50	0	2	1	1	**4**
X7R 0402 100nF 16V	500	32	1	0	1	5	**7**
X7R 0603 100nF 50V	500	100	0	1	0	0	**1**
C0G 0603 4.7nF 100V	500	200	0	0	0	0	**0**
C0G 1206 100nF 25V	500	50	0	0	1	1	**2**
X7R 1210 1µF 100V	500	200	0	2	2	1	**5**

Estimated Reliability

Since we have developed constants for activation energy and voltage coefficients for each of the selected part types, we can begin to predict FIT rates based on the formula in Equation 4. A high sample size life test of 500 pieces per batch was performed at two times rated voltage and rated temperature (125°C) on capacitors that were voltage conditioned. The accelerated life test failures were noted and included in the calculations using the FIT formula.

Reliability engineers commonly use FIT rates to estimate reliability. FIT rates are expressed in failures per billion piece hours. Using estimated FIT rates, we can make reliability predictions at the parts-per-billion and parts-per-million levels into future years of device service given application use conditions.

Table 7 depicts a summary of the application scenarios chosen to make reliability predictions. The application conditions used in the prediction model represent several potential use conditions in medical implantable and general medical electronic applications.

Table 7: Application Scenarios

Scenario	Application	Voltage	Temperature
1	Medical Implantable	Vr	37°C
2	Medical Implantable	50% Vr	37°C
3	Elevated Temperature	50% Vr	85°C

Vr = Rated Voltage

Given the varying scenarios, we can predict projected failure rates for the selected dielectric systems and their associated part numbers. Table 8 summarizes the C0G dielectric system reliability predictions.

Table 8: C0G FIT and Predicted Reliability

C0G Dielectric System					
KEMET Part Number	Scenario	FIT (Discrete)	Projected Failure Rate in 1 Year, Device (ppb)	Projected Failure Rate in 10 Years, Device (ppb)	Projected Failure Rate in 50 Years, Device (ppb)
C0G 1206 100nF 25V	1	2.49E-07	0.002	0.02	0.11
	2	1.54E-12	0.000	0.00	0.00
	3	1.66E-09	0.000	0.00	0.00
C0G 0402 1nF 25V	1	4.94E-05	0.433	4.3	22
	2	5.72E-10	0.000	0.000	0.000
	3	5.51E-08	0.000	0.005	0.024

For all three scenarios, the one-year projected failure rate is less than one part per billion (ppb) per device. The model requires 10 years for scenario one on the 0402 case size part number in order to reach a single digit ppb level of 4.3. This performance under rated voltage conditions and human body temperature demonstrates the robust reliability of this dielectric system for a medical implantable application. At elevated temperatures and half rated voltage, the ceramic capacitors are predicted not to fail at the ppb level with two significant figures.

Table 9 data depicts the predicted reliability of the BME X7R dielectric system. For all three scenarios, the one-year projected failure rate for 50V and 100V rated devices is less than one part per million (ppm) per device. For the 0402 case size 16V rated component, scenario 3 demonstrates a predicted ppm level of 17.5 in the first year. The Scenario 2 failure rate performance below 1ppm at 10 years of service life and at 50% rated voltage conditions and human body temperature demonstrates the robust nature of this dielectric system for a medical implantable application.

Table 9: X7R FIT and Predicted Reliability

X7R Dielectric System					
		FIT (Discrete)	Projected Failure Rate in 1 Year, Device (ppm)	Projected Failure Rate in 10 Years, Device (ppm)	Projected Failure Rate in 50 Years, Device (ppm)
X7R 0402 100nF 16V	1	1.31E-01	1.153	11.527	57.636
	2	9.44E-03	0.083	0.828	4.138
	3	2.14E+00	18.726	187.256	936.280
X7R 1210 1.0µF 100V	1	4.97E-03	0.044	0.435	2.176
	2	1.47E-05	0.000	0.001	0.006
	3	2.86E-03	0.025	0.251	1.254
X7R 0603 100nF 50V	1	3.04E-05	0.000	0.003	0.013
	2	7.21E-07	0.000	0.000	0.000
	3	4.23E-04	0.004	0.037	0.186

Conclusions

Previous studies on ceramic capacitor reliability point out the importance of defining voltage coefficients for accurate reliability modeling [12]. In this study there was a wide range of voltage coefficients varying from 3.8 to 17.3. In order to effectively predict reliability, it is important to develop the voltage coefficients to model capacitor behavior over known application conditions. The activation energy (E_a) values demonstrated a smaller range from 0.91 to 1.39. The effect of temperature is less significant than voltage on the time-to-failure for the capacitors modeled.

For the devices tested in this study, projected median time-to-failure is well in excess of 100,000 years for medical implantable application conditions at 50% rated voltage and 37°C. Projected failure rates for this application condition in the observed C0G dielectric system were practically zero ppb even up to 50 years of device use. Projected failure rates for this application condition in the observed X7R dielectric system were less than 1 ppm up to 10 years and less than 3.5 ppm up to 50 years.

As the pressure for higher reliability continues to increase for the Medical Electronics market, device manufacturers and capacitor suppliers must work in tandem to design-in the right capacitors under the known application conditions. When used under the proper application conditions, high-capacitance BME ceramic capacitors demonstrate excellent long-term reliability performance.

ACKNOWLEDGEMENTS
The authors would like to express gratitude to Ella Jones for conducting all the HALT tests, Jose Luis del Angel for preparing the samples, and Alicia Cruz for completing the Load Life testing. Special thanks to Bob Willoughby and Abhijit Gurav for their technical guidance and advice.

REFERENCES
[1] B. S. Rawal, M. Kahn, and W. R. Buessem, *Grain Boundary Phenomena in Electronics Ceramics* in Advances in Ceramics, Vol. 1, p. 172-188, 1981.
[2] D. Hennings and G. Rosenstein, *J. Am. Ceram. Soc.*, **67**, 249-254 (1984).
[3] Y. Mizuno, T. Hagiwara, H. Chazono, and H. Kishi, *J. Euro.Ceram. Soc*., **21**, 1649-1652 (2001).
[4] X. Xu, P. Pinceloup, J. Beeson, A. Gurav, and G.Y. Yang, p373-376, 12th US-Japan Seminar on Dielectric and Piezoelectric Ceramics, Nov. 6-9, 2005, Annapolis, MD, USA.
[5] X. Xu, et al., p179-188, CARTS USA 2007, Alburquerque, NM, USA.
[6] P. Pinceloup, et al., p459-466, CARTS USA 2006, Orlando, FL, USA.
[7] A. S. Gurav, X. Xu, P. Pinceloup, M. Sato, A. Tajuddin, C. Randall and G. Yang, 13th US-Japan Seminar on Dielectric and Piezoelectric Ceramics, Nov. 2-5, 2007, Awaji Island, Japan.
[8] T. Prokopowicz and A. Vaskas, "Research and Development, Intrinsic Reliability, Subminiature Ceramic Capacitors," Final Report, ECOM-9705-F, 1969 NTIS AD-864068
[9] G. Maher, "Highly Accelerated Life Testing of K-4500 Low Fired X7R Dielectric," Proceedings of the Passive Components for Power Electronics Workshop. April 26-27, 2000, Penn State University. Also presented in parts at the US-Japan Seminar on Dielectric Studies November, 1999, Okinawa, Japan.
[10] M.J. Cozzolino, B. Wong, L.S. Rosenheck, "Investigation of Insulation Resistance Degradation in BG Dielectric Characteristic, MIL-PRF-55681 Capacitors," CARTS 2001 pp. 254-264.
[11] J.L. Paulsen, E.K. Reed, "Highly Accelerated Life Testing of KEMET Base Metal Electrode (BME) Ceramic Chip Capacitors," CARTS 2001, pp. 265-270.
[12] M. Randall, A. Gurav, D. Skamser, J. Beeson, "Lifetime Modeling of Sub 2 Micron Dielectric Thickness BME MLCC," CARTS 2003.